Proceedings of the ASME 2017 International Design Engineering Technical Conferences and Computers and Information in Engineering Conference
IDETC/CIE 2017
August 6-9, 2017, Cleveland, Ohio, USA

DETC2017-68355

ANALYSIS OF MAXIMUM POSSIBLE SAMPLING PERIOD FOR A REAL-TIME VISION-BASED CONTROL SYSTEM

Bo Shang
College of Information Science and Engineering,
Northeastern University,
China, 110819,
Email: cnpcshangbo@gmail.com

Chengdong Wu *
Yunzhou Zhang
College of Information Science and Engineering,
Northeastern University,
China, 110819,
Email address (wuchengdong@ise.neu.edu.cn)

YangQuan Chen †
Mechatronics, Embedded Systems and Automation (MESA) Lab,
School of Engineering,
University of California, Merced,
CA, USA
Email address (ychen53@ucmerced.edu)

ABSTRACT

Drone control systems are experiencing more and more challenges when integrating with more sensors. For example, the drone visual servoing systems often have a large sampling period due to limited on-board computing capability. Therefore, controllers that can tolerate a large sampling period are needed. Our previous work showed that a fractional order proportional-derivative controller (FOPD controller) can tolerate a larger sampling period than an integer order proportional-integralderivative controller (IOPID controller). In this paper, we verified this conclusion using control system stability criteria to estimate the largest sampling periods and time-domain simulation.

1 INTRODUCTION

[1] talked about the challenges and bottleneck problems that UAS (Unmanned Aerial System) research is currently facing. Sensor signal processing is one of these challenges. [2] talked about the challenges the visual-based drone is facing.

In our previous work [3], we compared the performance of a fractional order proportional-derivative (FOPD) controller and integer order proportional-integralderivative (IOPID) controller for a drone visual-servoing application. At that time, we expected the FOPD controller to have a better performance in overshoot and rising time; however, we found that the FOPD controller can tolerate a larger sampling period than the IOPID controller in the simulation. We believe this is an important feature for drone visual-based control because the drones often have limited on-board computing capability.

A literature review has been done to prove that the FOPD controller can tolerate a larger sampling period than the IOPID controller theoretically. [4] discussed the maximum time delay of a control system for both fractional order controllers and integral order controllers. The author concluded that the fractional order controllers can be optimized to tolerate a larger time delay. Bhambhani's conclusion is similar to what we want, however, the difference is that they focused on the largest time delay, while we want to estimate the largest sampling period. Therefore, we believe we can use a similar method to estimate the largest sampling period. Bhambhani used Eriksson's tuning rule for varying time-delay systems [5] as an objective function of the formulated optimization problem.

We found some stability criteria that have taken the sampling period into account. [6]'s stability criterion is one of them, based on the small gain theorem. [7] further investigates the stability of a sampled-data system with variable sampling periods. Novel sampling-interval-dependent stability criteria are derived

*Mentor.
†Joint Mentor.

by a new Lyapunov-like functional approach that does not involve model transformation.

In this paper, we propose a method that can numerically estimate the largest sampling period that a controller can tolerate based on Kao's stability criterion and optimization method. By estimating the largest sampling period that a real-time vision-based control system can tolerate, we proved our previous supposition. Simulations have been done for both FOPD and IOPID controllers.

2 BASIC CONCEPT AND TERMINOLOGY

2.1 Real-time Vision-based Control System Model

This work is based on the control model in [3], which ignored the time delay. The model is shown in Figure 1. We considered the time delay in this article.

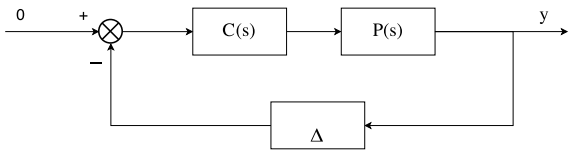

FIGURE 1. The control model for a real-time vision-based control system

2.2 FOPD Controller and Tuning Rules

The plant model is identified to be:

$$P(s) = \frac{K}{\tau s + 1}\frac{1}{s}, \tag{1}$$

where $K = 1.0263$, $\tau = 0.71$.

The frequency model of the FOPD controller is:

$$C(s) = K_p + K_d s^{\lambda}, \tag{2}$$

where K_p and K_d are the proportional and derivative gain parameters of the fractional controller, respectively, and λ is the noninteger order of the integrator.

The tuned FOPD controller is:

$$C_{FOPD}(s) = 0.6192 s^{0.9694} + 2.6992, \tag{3}$$

The tuned IOPID controller is:

$$C_{IOPID}(s) = 2.89 + \frac{1.04}{s} + 1.79 s, \tag{4}$$

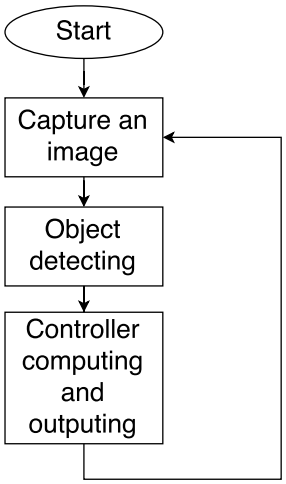

FIGURE 2. The vision-based control system working period

2.3 Sampled-data System Stability Criteria

For the drone vision-based control, the controller is a discrete system with a large sampling period. Therefore, the continuous model does not take the sampling into account. A CT-DT model (Continuous Time - Discrete Time model) can be more accurate in estimating the sampling period and taking the sampling into account. Theorem 2 in [8] gave us the following conclusion for CT-DT models.

For the closed loop system in Figure 1, with continuous-time, strictly proper, and stable $P(s)$, and discrete-time $C(z)$ sampled with a period of h seconds, the system is stable for any time-varying delays defined by

$$\Delta(v) = v(t\delta(t)), 0 \le \delta(t) \le Nh.$$

For some integer N, if

$$\left| \frac{P_{alias}(\omega)C(e^{j\omega})}{1 + P_{ZOH}(e^{j\omega})C(e^{j\omega})} \right| < \frac{1}{N\left|e^{j\omega}1\right|}, \forall \omega \in [0, \infty], \tag{5}$$

where $P_{ZOH}(z)$ is the ZOH discretization of $P(s)$, and

$$P_{alias}(\omega) = \sqrt{\sum_{k=\infty}^{\infty} \left| P(j(\omega + 2\pi k)\frac{1}{h}) \right|^2}.$$

For the drone vision-based control system, the system has a working period as shown in Figure 2.

3 PROBLEM FORMULATION

From Figure 2, we know that the sampling period is nearly the same as the time delay. Therefore, we assume that the sam-

pling period and the time delay are the same ($N = 1$).

We used the MATLAB function `c2d` [9] to compute the `ZOH` discretization of $P(s)$(Equation 1). When using `c2d`, a sampling period is selected. For example, when the sampling period $T = 0.1\mathtt{s}$, the `ZOH` discretization is:

$$P_{ZOH} = \frac{0.0069z + 0.006583}{z^2 - 1.869z + 0.8686}.$$

To get the maximum sampling period h, we need to get the maximum h when equation 6 is true. Because not only the h is used in $P_{alias}(\omega)$ and the discretization of $P_{ZOH}(e^{j\omega})$ and $C(e^{j\omega})$ but also the equation should be true for all $\omega \in [0, \infty]$, the mathematical relationship contains a lot of nonlinearity. Therefore, we formulated the process of computing the sampling period as an optimization problem, which can be solved by the MATLAB Global Optimization Toolbox [10]. The two input variables are frequency ω and sampling period h. Because we need to search for the maximum sampling period when the constraint (Equation 5) is met, the objective function is set to:

$$O(h) = -h.$$

The unequal constraint is:

$$f(h) = \max_{\omega \in [0,\text{inf}]} \left| \frac{P_{alias}(\omega)C(e^{j\omega})}{1 + P_{ZOH}(e^{j\omega})C(e^{j\omega})} \right| - \frac{1}{N|e^{j\omega} - 1|} < 0. \quad (6)$$

The initial state:

$$x_0 = 0.3.$$

The lower and upper bounds are:

$$lb = 10^{-5},$$

$$ub = 50.$$

Because the unequal constraint is difficult to calculate, we formulated the calculation of $f(h)$ as a separate optimization problem. The objective function is:

$$O(\omega) = -\left| \frac{P_{alias}(\omega)C(e^{j\omega})}{1 + P_{ZOH}(e^{j\omega})C(e^{j\omega})} \right| + \frac{1}{N|e^{j\omega} - 1|}.$$

The initial state:

$$\omega = 2.$$

The lower and upper bounds are:

$$lb = 10^{-5},$$

$$ub = 10^{4}.$$

4 MAXIMUM SAMPLING PERIOD ESTIMATION

Because the input variable can be nonintegral, we used the `fmincon` function in MATLAB to estimate the minimum value of the objective function $O(\omega)$.

4.1 IOPID Controller Maximum Sampling Period

Then, we plotted the objective function $f(h)$ to estimate the maximum sampling period h as shown in 3. This plot took 70.3 s on a Dell workstation to calculate those eight points, so we did not plot more points in this figure.

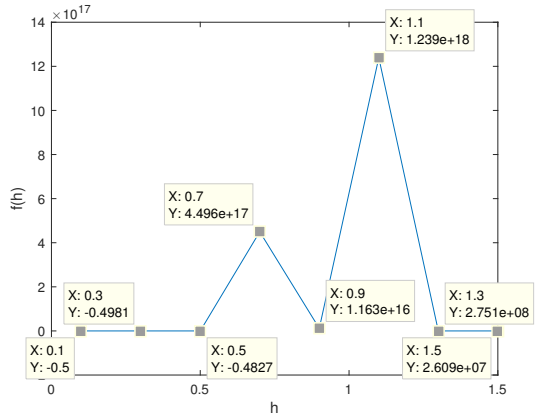

FIGURE 3. The function $f(h)$ when $h \in (0, 1.5]$

From Figure 3, we can see that when the sampling period h is small, the $f(h)$ is negative, which means the system is stable. When the sampling period becomes greater than a certain number, the $f(h)$ goes positive very quickly and never goes back to negative. Therefore, we computed more points for $h \in (0.5, 0.7)$ (Figure 4) to estimate the largest sampling period h_{max}. We noticed that Figure 4 and Figure 3 have a similar pattern. The h_{max} is supposed to be between 0.5 s and 0.5571 s. By repeating the

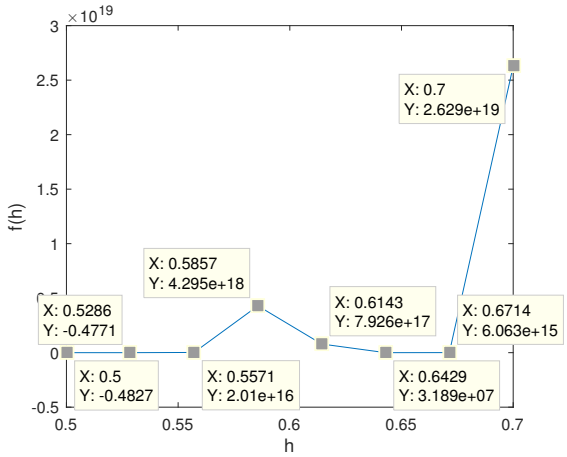

FIGURE 4. The function $f(h)$ when $h \in (0.5, 0.7)$

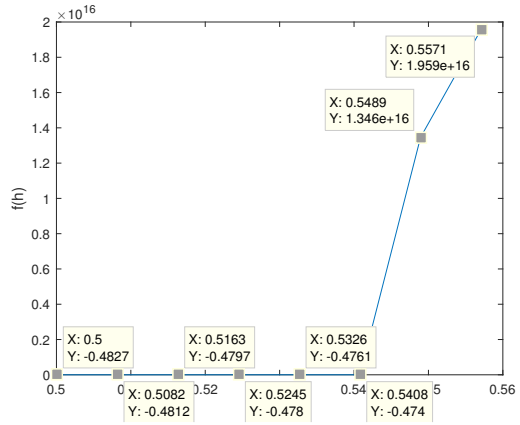

FIGURE 5. The function $f(h)$ when $h \in (0.5, 0.5571)$

same plotting method, we plotted Figure 5 to show the value of $f(h)$ when $h \in (0.5, 0.5571)$. From Figure 5, we found the h_{max} should be between 0.5408 s and 0.5489 s. Therefore, we plotted Figure 6 and finally found for the IOPID system, the maximum sampling period is:

$$h_{\max}(\text{IOPID}) = 0.55 \text{ s}. \tag{7}$$

4.2 FOPD Controller Maximum Sampling Period

For the FOPD controller, we used the Oustaloup method [11] to convert the fractional order part $s^{0.9694}$ to a high-order

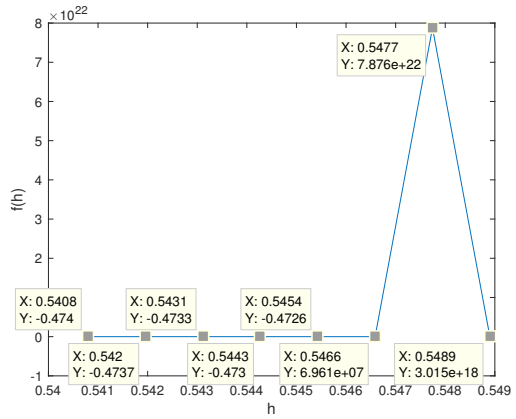

FIGURE 6. The function $f(h)$ when $h \in (0.5454, 0.5466)$

integer order transfer function:

$$\begin{aligned} s^{0.9694} \approx (&809.5s^9 + 2.276e06s^8 + 1.134e09s^7 + 1.173e11s^6 \\ &+ 2.592e12s^5 + 1.232e13s^4 + 1.258e13s^3 + 2.748e12s^2 \\ &+ 1.245e11s + 1e09)/(s^9 + 1.245e04s^8 + 2.748e07s^7 \\ &+ 1.258e10s^6 + 1.232e12s^5 + 2.592e13s^4 + 1.173e14s^3 \\ &+ 1.134e14s^2 + 2.276e13s + 8.095e11). \end{aligned} \tag{8}$$

The parameters are selected as in Table 1.

TABLE 1. Oustaloup parameters

Parameters	Meanings	Values
w_L	Low frequency limit	$\omega_c/1000$
w_H	Upper frequency limit	$100\omega_c$
r	Fractional order	0.9694
N	Order of the finite TF approximation	4

We used a similar method to estimate the maximum sampling period of the FOPD control system. A MATLAB function `c2d` command was used to convert the plant model (Equation 1) and the fractional controller model (Equation 2) to a discrete transfer function. Then Equation (6) was used to calculate the unequal constraint function $f(h)$.

The $f(h)$ is plotted against different $h \in [0.1, 10]$ (Figure 7) From Figure 7, we found $h_{max} \in (0.1, 1.514)$. Then we plotted $f(h)$ when $h \in (0.1, 1.514)$ (Figure 8).

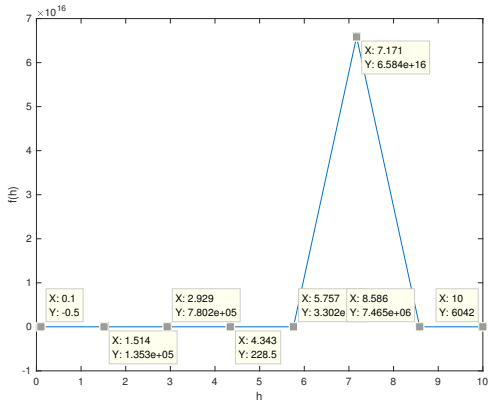

FIGURE 7. The function $f(h)$ when $h \in [0.1, 10]$

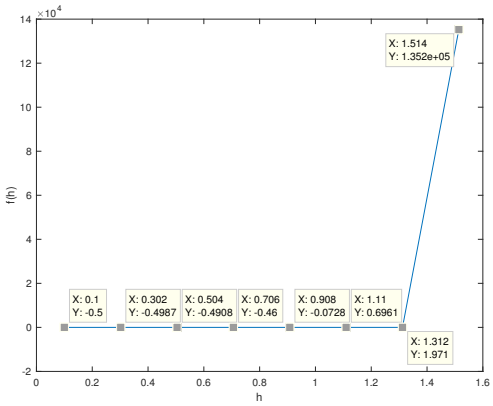

FIGURE 8. The function $f(h)$ when $h \in [0.1, 1.514]$

From Figure 8, we found $h_{\max} \in (0.908, 1.11)$. Then, we plotted $f(h)$ when $h \in [0.908, 1.11]$ (Figure 9).

From Figure 9, we found the maximum sampling period of the FOPD system is:

$$h_{\max}(\text{FOPD}) = 0.908 \text{ s}. \tag{9}$$

Obviously, the FOPD system has a larger sampling period than the IOPID system.

5 TIME-DOMAIN SIMULATION VERIFICATION

5.1 Integral Time-weighted Absolute Error (ITAE) Criterion Comparison

Several tuning methods based on minimizing the integrated absolute error (IAE) or integrated squared error (ISE) are com-

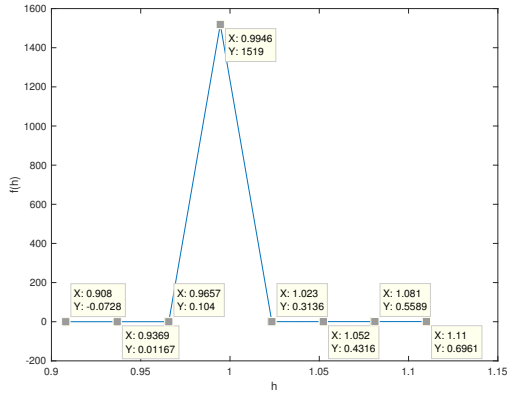

FIGURE 9. The function $f(h)$ when $h \in [0.908, 1.11]$

monly used [12]:

$$IAE = \int : e(t) : dt, ITAE = \int t : e(t) : dt$$

$$ISE = \int e(t)^2 dt, ITSE = \int te(t)^2 dt$$

We used ITAE to compare the IOPID (4) and FOPD (3) con-

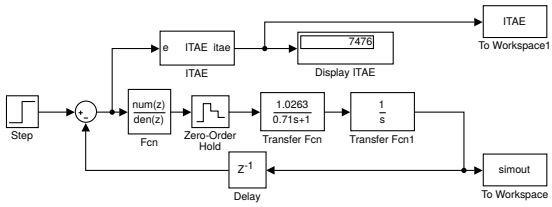

FIGURE 10. Using simulation to calculate the ITAE index

trollers. MATLAB SIMULINK was used to make a simulation system (Figure 10) for the IOPID and FOPD systems to get estimates of the ITAE values for different sampling periods. However, the formula to calculate the ITAE uses an infinite integral.

Because the infinite integral in the ITAE formula is not realizable, we used a definite integral instead.

$$ITAE = \int_0^{t_{end}} t : e(t) : dt$$

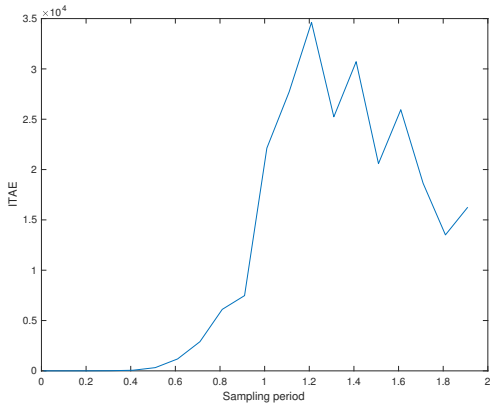

FIGURE 11. The ITAE index for different sampling periods (s) (IOPID)

where t_{end} denotes the simulation length. The simulation time was set to 10 s. The ITAE SIMULINK model is from [13].

From Figure 11, we notice the ITAE index of the IOPID system gets large rapidly after the maximum sampling period, which is around 0.55 s.

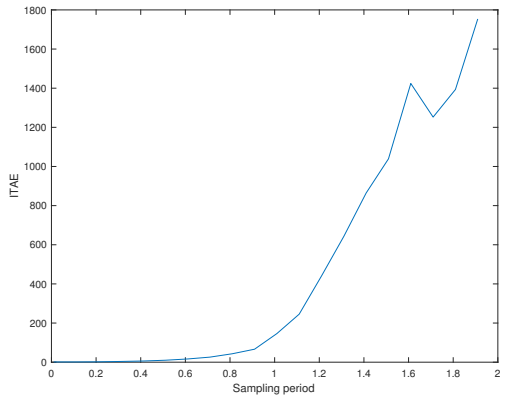

FIGURE 12. The ITAE index for different sampling periods (s) (FOPD)

From Figure 12, we notice that the ITAE index of the FOPD system gets large rapidly after the maximum sampling period, which is around 0.92 s.

6 CONCLUSION & FUTURE WORKS

This paper analyzed the maximum sampling period of a real-time vision-based control system. The maximum sampling period of the system was estimated using stability criteria and an optimization method for both the integer order proportional-integral-derivative controller case and the fractional order proportional-derivative controller case. The fractional order controller is proved to have a larger sampling period than the integer order controller when maintaining the same performance.

Future work should employ sampling-interval-dependent stability criteria [14] to estimate the maximum sampling period, using a multiobjective optimization method to design fractional order controllers that can tolerate a larger sampling period [15] [16], compare sampling periods for more plants [15] [17], and try to do real experiments to verify the estimated sampling period.

ACKNOWLEDGMENT

This work was supported by the China Scholarship Council, National Natural Science Foundation of China (No. 61273078, 61471110), Foundation of Liaoning Educational Commission (L2014090).

REFERENCES

[1] Kanellakis, C., and Nikolakopoulos, G., 2017. "Survey on Computer Vision for UAVs: Current Developments and Trends". *Journal of Intelligent & Robotic Systems*, Jan., pp. 1–28.

[2] Engel, J., Sturm, J., and Cremers, D., 2012. "Camera-based navigation of a low-cost quadrocopter". In 2012 IEEE/RSJ International Conference on Intelligent Robots and Systems, pp. 2815–2821.

[3] Shang, B., Liu, J., Zhao, T., and Chen, Y., 2016. "Fractional order robust visual servoing control of a quadrotor UAV with larger sampling period". In 2016 International Conference on Unmanned Aircraft Systems (ICUAS), pp. 1228–1234.

[4] Bhambhani, V., Chen, Y., and Xue, D., 2008. "Optimal fractional order proportional integral controller for varying time-delay systems". *IFAC Proceedings Volumes,* ***41***(2), pp. 4910–4915.

[5] Eriksson, L. M., and Johansson, M., 2007. "Simple pid tuning rules for varying time-delay systems". In Decision and Control, 2007 46th IEEE Conference on, IEEE, pp. 1801–1807.

[6] Kao, C.-Y., and Lincoln, B., 2004. "Simple stability criteria for systems with time-varying delays". *Automatica,* ***40***(8), pp. 1429–1434.

[7] Shao, H., Zhao, J., and Zhang, D., 2017. "Novel stability criteria for sampled-data systems with variable sampling periods". *IEEE/CAA Journal of Automatica Sinica*.

[8] Kao, C.-Y., and Lincoln, B., 2004. "Simple stability criteria for systems with time-varying delays". *Automatica,* ***40***(8), Aug., pp. 1429–1434.

[9] c2d. https://www.mathworks.com/help/control/ref/c2d.html. Accessed: 2017-02-16.

[10] Global optimization toolbox. https://www.mathworks.com/help/gads/index.html?searchHighlight=global%20optimization%20toolbox&s_tid=doc_srchtitle. Accessed: 2017-02-16.

[11] Oustaloup-Recursive-Approximation for Fractional Order Differentiators - File Exchange - MATLAB Central. http://www.mathworks.com/matlabcentral/fileexchange/3802-oustaloup-recursive-approximation-for-fractional-order-differentiators. Accessed: 2017-02-16.

[12] Dorf, R., and Bishop, R., 1998. "Modern Control Systems, 8th edition". *Books by Marquette University Faculty*, Jan.

[13] Simulink library Performance index. https://www.mathworks.com/matlabcentral/fileexchange/17287-simulink-library--performance-index. Accessed: 2017-02-16.

[14] Shao, H., Zhao, J., and Zhang, D., 2017. "Novel stability criteria for sampled-data systems with variable sampling periods". *IEEE/CAA Journal of Automatica Sinica,* ***PP***(99), Jan., pp. 1–6.

[15] Bhambhani, V., 2008. "Optimal Fractional Order Proportional And Integral Controller For Processes With Random Time Delays". PhD thesis, Citeseer.

[16] Bhambhani, V., Chen, Y., and Xue, D., 2008. "Optimal Fractional Order Proportional Integral Controller for Varying Time-Delay Systems". *IFAC Proceedings Volumes,* ***41***(2), pp. 4910–4915.

[17] Badri, V., and Tavazoei, M. S., 2013. "On tuning fractional order [proportionalderivative] controllers for a class of fractional order systems". *Automatica,* ***49***(7), July, pp. 2297–2301.